Synthesis and Characterization of Fluorine-Containing Liquid Crystalline Polysiloxanes Bearing Cholesteryl Cinnamate Mesogens and Trifluoromethyl-Substituted Mesogens

Fan-Bao Meng, Zheng-Yan Wang, Guo-Wei Chai, Hong-Guang Wang, Ying Chen, Bao-Yan Zhang

Centre for Molecular Science and Engineering, Northeastern University, Shenyang 110004, People's Republic of China

Received 18 December 2008; accepted 11 November 2009
DOI 10.1002/app.31760
Published online 14 January 2010 in Wiley InterScience (www.interscience.wiley.com).

ABSTRACT: Several novel side-chain liquid crystalline (LC) polysiloxanes bearing cholesteryl cinnamate mesogens and trifluoromethyl-substituted mesogens were synthesized by a one-step hydrosilylation reaction with poly(methylhydrogeno)siloxane, a cholesteric LC monomer cholesteryl 3-(4-allyloxy-phenyl)-acryloate and a fluoro-containing LC monomer 4-[2-(3-trifluoromethyl-phenoxy)-acetoxy]-phenyl 4-allyloxy-benzoate. The chemical structures and LC properties of the monomers and polymers were characterized by use of various experimental techniques, such as FTIR, ^{1}H-NMR, ^{13}C-NMR, TGA, DSC, POM, and XRD. The temperatures at which 5% weight loss occurred were greater than 300°C for all the polymers, and the residue weight near 600°C increased slightly with increase of the trifluoromethyl-substituted mesogens in the fluorinated polymer systems. The samples containing mainly cholesteryl cinnamate mesogens showed chiral nematic phase when they were heated and cooled, but the samples containing more trifluoromethyl-substituted mesogens exhibited chiral smectic A mesophase. The glass transition temperature of the series of polymers increased slightly with increase of trifluoromethyl-substituted mesogens in the polymer systems, but mesophase–isotropic phase transition temperature did not change greatly. In XRD curves, the intensity of sharp reflections at low angle increased with increase of trifluoromethyl-substituted mesogens in the fluorinated polymers systems, indicating that the smectic order derived from trifluoromethyl-substituted mesogens should be strengthened. These results should be due to the fluorophobic effect between trifluoromethyl-substituted mesogens and the polymer matrix. © 2010 Wiley Periodicals, Inc. J Appl Polym Sci 116: 2384–2395, 2010

Key words: liquid crystalline polymers (LCP); fluoropolymers; phase behavior; polysiloxanes

INTRODUCTION

Side-chain liquid crystalline polymers (SCLCPs) have been the subject of much interest for both fundamental and applied reasons. On the one hand, SCLCPs exhibit richer self-assembly characteristics that manifest an interplay between the backbone polymer matrix and liquid crystalline ordering between side chain rod units. On the other hand, some functional groups have been introduced to the SCLCPs, leading to functional materials. Some of these functional groups include azobenzene,[1–3] photochromic dyes,[4,5] spironaphthoxazine,[6] 1,3,4-oxadiazole,[7,8] and so on.

Introduction of chiral functional groups to SCLCPs has become one of the most important and complex topics in liquid crystal research recently. Chiral SCLCPs may exhibit a marvelous variety of mesophases, including the blue phases (BP*), the cholesteric phase (N*), and the chiral smectic C* phase (S$_{C}^{*}$).[9–11] SCLCPs showing S$_{C}^{*}$ phases have attracted both industrial and scientific interests because of their additional properties, such as piezoelectricity, ferroelectricity, and pyroelectricity resulting from the symmetry breaking brought by molecular chirality.[12–14]

Introduction of fluorine-containing units to SCLCPs leads to new functional materials. In polymer systems, fluorine's small size, large electronegativity, low polarizability, and large fluorine–fluorine repulsion lead to many interesting properties of fluoropolymers. The presence of fluorine atoms

Correspondence to: F.-B. Meng (fanbaomeng@hotmail.com) or B.-Y. Zhang (byzcong@163.com).

Contract grant sponsor: National Natural Science Foundation of China; contract grant number: 50873018.

Contract grant sponsors: China Postdoctoral Science Foundation, Program for New Century Excellent Talents in University.

strongly affects the hydrophobicity, oleophobicity, and critical micellar concentration.[15] Although fluoropolymers have long been known as an important class of functional materials, fluorinated SCLCPs are a relatively new class of fluoropolymers.[16–26]

Now we are interested in the kind of SCLCPs containing both chiral functional groups and fluorine-containing units. These new macromolecular architectures might provide new functional materials. It is also necessary to know the effect of the both functional groups on behaviors of SCLCPs. In this article, we synthesized a series of SCLCPs bearing chiral cholesteryl cinnamate mesogens and trifluoromethyl-substituted mesogens by use of poly(methylsiloxane) as main chains.

EXPERIMENTAL

Materials

3-Trifluoromethyl-phenol, 4-hydroxybenzoic acid, benzene-1,4-diol, 2-chloro-acetic acid, 3-(4-hydroxy-phenyl)-acrylic acid, 3-bromopropene, cholesterol, *N*,*N*-dimethyl formamide (DMF), poly(methylhydrogeno)siloxane (PMHS) (M_n = 580) and hexachloroplatinic acid hydrate were obtained from Jilin Chemical Industry Company and used without any further purification. Pyridine, acetone, toluene, chloro-benzene, thionyl chloride, chloroform, ethanol, tetrahydrofuran (THF), and methanol were purchased from Shenyang Chemical Co. Toluene was used in the hydrosilation reaction over sodium and then distilled under nitrogen. Pyridine was purified by distillation over KOH and NaH before using.

Characterization

FTIR spectra of the synthesized monomers and polymers were obtained by the KBr method performed on PerkinElmer instruments Spectrum One Spectrometer (PerkinElmer, Foster City, CA). ^{1}H-NMR (300 MHz) spectrum was obtained with a Varian Gemini 300 NMR Spectrometer (Varian Associates, Palo Alto, CA) with tetramethylsilane (TMS) as an internal standard. ^{13}C-NMR (600MHz) spectrum was obtained with a Bruker AV-600 NMR Spectrometer (Bruker, Fällanden, Switzerland). Thermal behaviors were characterized by use of a NETZSCH TGA 209C thermogravimetric analyzer, and a NETZSCH instruments DSC 204 (Netzsch, Wittelsbacherstr, Germany) at a heating rate of 10°C min^{-1} under nitrogen atmosphere. X-ray diffraction (XRD) measurements of the samples were performed using Cu Kα(λ = 1.542 Å) radiation monochromatized with a Rigaku DMAX-3A X-ray diffractometer (Rigaku, Japan). Polarizing optical microscopic (POM) observation of liquid crystalline transitions and optical textures was made using a Leica DMRX (Leica, Wetzlar, Germany) microscope with crossed polarizers and equipped with a Linkam THMSE-600 (Linkam, Surrey, England) hot stage. Measurement of optical rotation was carried out with a PerkinElmer instrument Model 341 polarimeter using the D line of a sodium vapor lamp.

Synthesis

The synthetic routes to liquid-crystalline monomers cholesteryl 3-(4-allyloxy-phenyl)-acryloate (**M1**) and 4-[2-(3-trifluoromethyl-phenoxy)-acetoxy]-phenyl 4-allyloxy-benzoate (**M2**) were shown in Scheme 1.

3-Bromopropene (24.3 g, 0.21 mol) and 3-(4-hydroxy-phenyl)-acrylic acid (32.8 g, 0.20 mol) were dissolved in 100 mL ethanol. It was stirred and added dropwise with solution of potassium

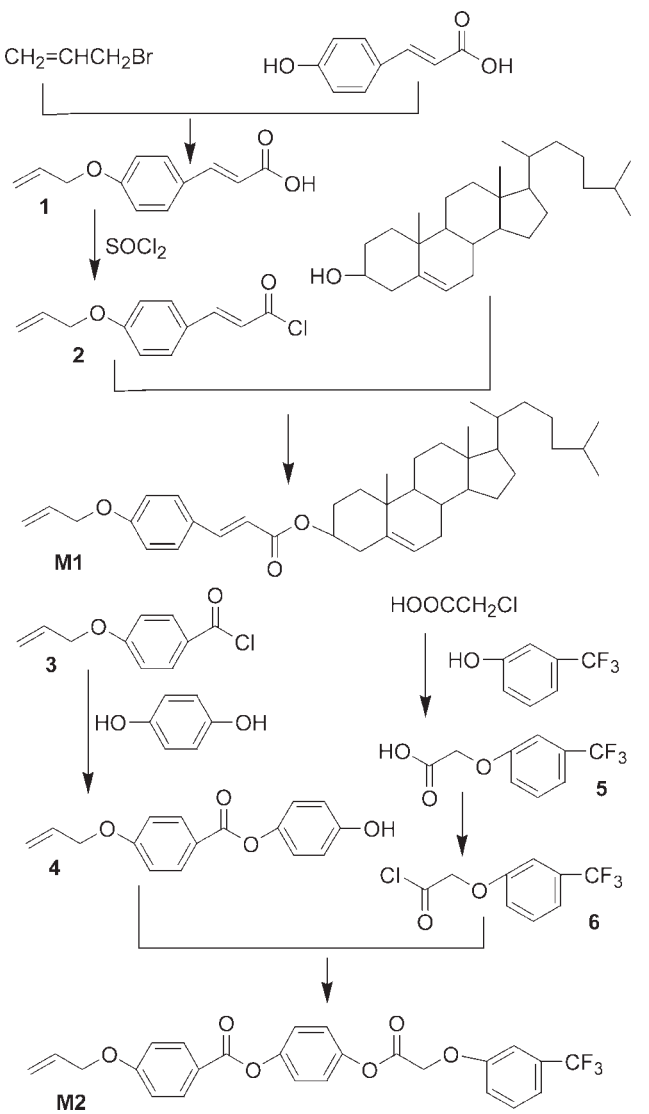

Scheme 1 Synthetic routes to monomers cholesteryl 3-(4-allyloxy-phenyl)-acryloate (**M1**) and 4-[2-(3-trifluoromethyl-phenoxy)-acetoxy]-phenyl 4-allyloxy-benzoate (**M2**).

hydroxide (44.0 g, 0.79 mol) and 0.3 g potassium iodide that were dissolved in 60 mL water. The reaction mixture was stirred at 80°C for 18 h. After cooling to room temperature, the mixture was poured into 100 mL cold water and acidified with 6*N* sulfuric acid. The precipitates were isolated by filtration and dried in a vaccum oven. 33.0 g of white crystals of 3-(4-allyloxy-phenyl)-acrylic acid (**1**) was obtained after several recrystallizations from ethanol (yield: 81%), mp 160–161°C.

FTIR (KBr, cm^{-1}): 3085, 2926, 2868 (—CH_2—, CH_2=, and =CH), 2608–2503 (—OH in —COOH), 1692 (C=O in —COOH), 1602, 1509 (Ar), 1251, 1172 (C—O—C). ^{1}H-NMR (300 MHz, $CDCl_3$) δ = 4.60 (*d*, *J* = 6.2 Hz, 2H, =CH—CH_2—O—), 5.34 (d, *J* = 18.0 Hz, 2H, CH_2=CH—), 6.01–6.08 (*m*, 1H, CH_2=C*H*—), 6.39 (d, *J* = 16.0 Hz, 1H, —CH=C*H*—COO—), 6.81 (d, *J* = 8.2 Hz, 2H, Ar—*H*), 7.19 (d, *J* = 8.4 Hz, 2H, Ar—*H*), 7.63 (d, *J* = 16.1 Hz, 1H, —C*H*=CH—COO—), 11.2 ppm (*s*, —COO*H*). ^{13}C-NMR (600 MHz, $CDCl_3$): δ = 75.8 (—O—CH_2—); 114.1 (Ar—C); 115.1 (CH_2—CH—); 116.9 (—CH=CHCOO—); 127.2, 128.3 (Ar—C); 136.7 (CH_2=CH—); 145.3 (—CH=CHCOO—); 161.2 (—O—Ar—C); 169.7 ppm (—CH=CHCOOH).

The intermediate compound **1** (20.4 g, 0.10 mol), 1.00 mL of DMF and 70 mL thionyl chloride were added into a round flask equipped with an absorption instrument of hydrogen chloride. The mixture was stirred at room temperature for 1 h, then heated to 60°C and kept for 12 h. The excess thionyl chloride was distilled under reduced pressure. After cooling to room temperature, the residue was added with 40 mL cold chloroform to obtain chloroform solution of 3-(4-allyloxy-phenyl)-acryloyl chloride (**2**). Cholesterol (38.7 g, 0.10 mol) and 60 mL pyridine was dissolved in 120 mL chloroform to form a solution. The chloroform solution of **2** was added dropwise to the solution and reacted at 60°C for 13 h; then the chloroform was distilled out. The reaction mixture was cooled, poured in 1000 mL of cold water and acidified with 6*N* sulfuric acid solution. The precipitated crude product was filtered, dried overnight under vacuum to obtain a brown powder. Recrystallization in component solvent (100 mL ethanol and 100 mL THF) resulted in 44.6 g of flavescent crystals of liquid crystalline monomer cholesteryl 3-(4-allyloxy-phenyl)-acryloate (**M1**, yield: 78%), mp 147–148°C.

FTIR (KBr, cm^{-1}): 2937, 2867, 2850 (CH_3— and —CH_2—), 1710 (C=O), 1604, 1511 (Ar), 1287, 1256, 1176 (C—O—C). ^{1}H-NMR (300 MHz, $CDCl_3$): δ = 0.69–2.01 (m, 41H, —CH_3, —CH_2—, and —C*H*— in cholesteryl groups), 2.40 (*d*, *J* = 7.6 Hz, 2H, —O—CH—CH_2—C= in cholesteryl groups), 4.57 (d, *J* = 6.6 Hz, 2H, =CH—CH_2—O—), 4.72–4.75 (m, 1H, —O—C*H*— in cholesteryl groups), 5.29–5.33 (*m*, 1H, =C*H*— in cholesteryl groups), 5.43 (d, *J* = 18.6 Hz, 2H, CH_2=CH—), 6.01–6.09 (m, 1H, CH_2=C*H*—), 6.30 (d, *J* = 15.9 Hz, 1H, —CH=C*H*—COO—), 6.91 (d, *J* = 8.7 Hz, 2H, Ar—*H*), 7.47 (d, *J* = 8.4 Hz, 2H, Ar—*H*), 7.62 ppm (d, *J* = 15.9 Hz, 1H, —C*H*=CH—COO—). ^{13}C-NMR (600 MHz, $CDCl_3$): δ = 11.8, 21.0, 22.5, 22.8, 23.8, 24.2, 27.9, 28.0, 28.2, 31.8, 31.9, 35.7, 36.1, 36.6, 37.0, 38.2, 39.5, 39.7, 42.3, 50.0, 56.1, 56.6 (CH_3—, —CH_2—, and —CH— in cholesteryl groups); 68.8 (—O—CH_2—); 73.8 (—O—CH— in cholesteryl groups); 115.0 (Ar—C); 116.2 (CH_2=CH—); 117.9 (—CH=CHCOO—); 122.6 (—C=CH— in cholesteryl groups); 127.4 (Ar—C); 129.6 (Ar—C); 132.7 (CH_2=CH—); 139.7 (—CH=CHCOO—); 144.0 (—C=CH— in cholesteryl groups); 160.2 (Ar—C); 166.7 ppm (—CH=CHCOO—).

4-Allyloxy-benzoyl chloride (**3**) was synthesized according to a reported procedure.[27] Benzene-1,4-diol (44.0 g, 0.40 mol) and 8 mL pyridine were dissolved in 150 mL THF. It was added dropwise with **3** (19.6 g, 0.10 mol) and stirred at room temperature for 1 h. The reaction mixture was then stirred at 60°C for 6 h. After cooling to room temperature, the mixture was poured into 1000 mL cold water and acidified with 6*N* sulfuric acid. The precipitates were washed with hot water to remove the excess benzene-1,4-diol, isolated by filtration and dried in a vaccum oven. 21.3 g of white crystals of 4-hydroxy-phenyl 4-allyloxy-benzoate (**4**) was obtained after several recrystallizations from acetone (yield: 79%), mp 159–160°C.

FTIR (KBr, cm^{-1}): 3426 (—OH), 3060, 2928, 2850 (=CH_2, =CH—, and —CH_2), 1706 (C=O), 1608, 1509 (Ar), 1288, 1164 (C—O—C). ^{1}H-NMR (300 MHz, $CDCl_3$): δ = 4.61 (d, *J* = 5.8 Hz, 2H, =CH—CH_2—O—), 5.26 (d, *J* = 18.0 Hz, 2H, CH_2=CH—), 5.93–6.01 (m, 1H, CH_2=C*H*—), 6.89–7.16 (*m*, 6H, Ar—*H*), 8.11 (d, *J* = 6.2 Hz, 2H, Ar—*H*), 10.2 ppm (*s*, 1H, Ar—O*H*). ^{13}C-NMR (600 MHz, $CDCl_3$): δ = 75.4 (=CH—CH_2—O—); 115.1 (CH_2=CH—); 114.2, 116.1, 122.8, 122.9, 131.2 (Ar—C); 132.4 (CH_2=CH—); 145.8, 154.1, 167.2 (—O—Ar—C); 164.0 ppm (Ar—COO—).

Sodium hydroxide (8.4 g, 0.21 mol) and 3-trifluoromethyl-phenol (32.4 g, 0.20 mol) were dissolved in 100 mL chloro-benzene. The reaction mixture was stirred at 85°C for 3 h. It was added dropwise with 2-chloro-acetic acid (9.4 g, 0.10 mol) that was dissolved in 25 mL chloro-benzene, and stirred at 115°C for 2 h to ensure that the reaction finished. The solvent chloro-benzene was distilled under reduced pressure. After cooling to room temperature, the residue was poured into 50 mL cold water and acidified with 6*N* sulfuric acid. The precipitates were washed with water, isolated by filtration, and dried in a vaccum oven. Recrystallization in ethanol results in 19.6 g of white crystals of

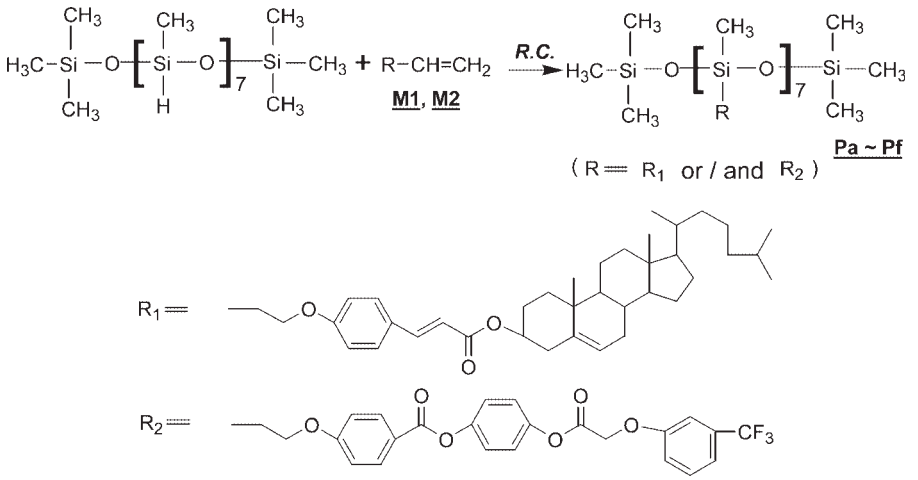

Scheme 2 Synthetic route to polymers **Pa–Pf**. Reagents and conditions (R.C.): H_2PtCl_6 / tetrahydrofuran, 65°C.

(3-trifluoromethyl-phenoxy)-acetic acid (**5**, yield: 89%), mp 95–96°C.

FTIR (KBr, cm^{-1}): 3300–2500 (—OH in —COOH), 2954, 2852 (=CH—, —CH_2—), 1740 (C=O), 1605, 1508 (Ar), 1253, 1167 (C—O—C), 1126 (C—F). ^{1}H-NMR (300 MHz, $CDCl_3$): δ = 4.89 (*s*, —OOC*CH*$_2$—O—), 6.79–7.32 (*m*, 4H), 11.1 ppm (*s*, *H*OOCCH$_2$O—). ^{13}C-NMR (600 MHz, $CDCl_3$): δ = 75.2 (—OOCCH$_2$O—); 111.0, 117.4, 117.6, 129.7, 132.1 (Ar—C); 119.7 (—CF_3); 162.4 (—O—Ar—C); 175.6 ppm (—OOCCH$_2$O—).

The intermediate **5** (7.0 g, 0.032 mol), 20 mL thionyl chloride and 1.0 mL of DMF were added into a round flask equipped with an absorption instrument of hydrogen chloride. The mixture was stirred at room temperature for 1 h, then heated to 60°C and kept for 6 h. The excess thionyl chloride was distilled out under reduced pressure to obtain 6.8 g of (3-trifluoromethyl-phenoxy)-acetyl chloride (**6**).

To a solution of compound **4** (5.4 g, 0.020 mol), pyridine (2.0 mL) and 35 mL of dry THF were added dropwise compound **6** (5.0 g, 0.021 mol) at 25°C. The mixture was stirred at room temperature under dry air for 2 h, refluxed for 7 h, and poured into 200 mL of ice water and acidified with 6*N* sulfuric acid. 7.8 g of white solid 4-[2-(3-trifluoromethyl-phenoxy)-acetoxy]-phenyl 4-allyloxy-benzoate (**M2**) was obtained after several recrystallizations from acetone (yield: 83%), mp 115–116°C.

FTIR (KBr, cm^{-1}): 3080, 2929 (=CH_2, =CH—), 1762, 1723 (C=O in different ester linkage), 1607, 1511 (Ar), 1283, 1169 (C—O—C), 1122 (C—F). ^{1}H-NMR (300 MHz, $CDCl_3$): δ = 4.64 (d, *J* = 5.2 Hz, 2H, =—CH—C*H*$_2$—O—), 4.94 (s, —OOCC*H*$_2$—O—), 5.45 (dd, *J* = 18.7 Hz, 2H, C*H*$_2$=CH—), 6.03–6.09 (m, 1H, CH_2=C*H*—), 6.99–7.46 (m, 10H, Ar—*H*), 8.14 ppm (d, *J* = 6.0 Hz, 2H, Ar—*H*). ^{13}C-NMR (600 MHz, $CDCl_3$): δ = 65.4 (—OOCCH$_2$O—); 68.9 (=CH—CH_2—O—); 114.5 (CH_2=CH—); 111.8, 118.1, 118.2, 118.7, 121.6, 122.0, 122.8, 130.2, 132.2 (Ar—C); 119.5 (—CF_3); 132.3 (CH_2=CH—); 147.2, 148.8, 157.7, 164.6 (—O—Ar—C); 163.0 (Ar—COO—); 166.7 ppm (—OOCCH$_2$O—).

For synthesis of polymers **Pa–Pf**, the same method was adopted, and the synthetic route were shown in Scheme 2. The polymerization experiments were summarized in Table I. The synthesis of polymer **Pc** was given as an example. Liquid crystalline monomer **M1** (1.71 g, 3.0 mmol) and fluorinated liquid crystalline monomer **M2** (0.47 g, 1.0 mmol) was dissolved in 25 mL of dry, fresh distilled toluene. To the stirred solution, PMHS (0.31 g, 0.54 mmol) and 2 mL of a 0.2% solution of hexachloroplatinic acid in THF were added and heated under nitrogen and anhydrous conditions at 65–68°C for 30 h. After this reaction time the FTIR analysis showed that the hydrosilation reaction was complete. Then the mixture was cooled and poured into 100 mL methanol. The polymers were separated and purified by several reprecipitations from tetrahydrofuran solution into methanol, and then dried at 80°C under vacuum for 24 h to obtain 1.93 g of polymer **Pc**.

FTIR (KBr, cm^{-1}): 2930, 2855 (C—H aliphatic), 1765–1710 (C=O in different ester linkages), 1606, 1509 (Ar), 1270, 1167 (C—O—C), 1129 (C—F), 1066 (Si—O). ^{1}H-NMR (300 MHz, $CDCl_3$): δ = 0–0.25 (m, 2.73H, Si—C*H*$_3$); 0.68 (m, 1.05H, Si—C*H*$_2$—); 0.86–2.31 (m, 16.01H, alkyl-*H*); 4.18–4.29 (m, 1.00H, —OC*H*$_2$CH$_2$—); 4.72–4.76 (*m*, 0.34H, —O—C*H*— in cholesteryl groups); 4.91–4.96 (*m*, 0.32H, —OOCC*H*$_2$—O—); 5.31–5.39 (*m*, 0.36H, =C*H*— in cholesteryl groups); 6.31–6.39 (*m*, 0.35H, —CH=C*H*—COO—); 6.9–8.26 ppm (m, 3.49H, Ar—H).

RESULTS AND DISCUSSIONS

Structural characterization

Liquid crystalline monomers **M1** and **M2** were prepared by esterification of hydroxyl group and acyl

TABLE I
Polymerization, Component Analyses, Specific Rotation, and X-Ray Data of the Side-Chain Polysiloxanes

Sample	Feed			M_n[a]	Fluorinated mesogens[b] (%)	Specific rotation[c]	d-spacing[d] (Å)
	PMHS (mmol)	M1 (mmol)	M2 (mmol)				
Pa	0.54	4.0	0	4650	0	−18.1	31.5[e], 5.47
Pb	0.54	3.5	0.5	4530	8.3	−15.0	32.2[e], 5.44
Pc	0.54	3.0	1.0	4410	17.1	−14.9	33.9, 5.43
Pd	0.54	2.5	1.5	4330	26.1	−14.3	35.3, 5.33
Pe	0.54	2.0	2.0	4220	35.5	−13.1	37.2, 5.27
Pf	0.54	1.5	2.5	4050	45.4	−12.5	40.1, 5.15

[a] Based on the starting poly(methylhydrogeno)siloxanes and polymer composition of the polymers from ^{1}H-NMR spectra.
[b] Mass percentage of trifluoromethyl-substituted mesogens in the polymers, derived from the starting poly(methylhydrogeno)siloxanes and polymer composition according to ^{1}H-NMR spectra analysis.
[c] Specific rotation of polymers ($[\alpha]_D^{20}$), 0.1 g in 50 mL toluene.
[d] X-ray diffraction (XRD) peaks of samples.
[e] These diffractions are wide and diffuse.

chloride in the presence of pyridine in organic solvents such as chloroform and THF. The chemical structures of **M1** and **M2** were characterized with FTIR, ^{1}H-NMR, and ^{13}C-NMR spectra. The FTIR absorption range of the C=O stretching modes lies in 1710 cm^{-1} in **M1**, but the stretching bands of C=O in the reactant 3-(4-allyloxy-phenyl)-acryloyl chloride is found at 1760 cm^{-1}, indicating that esterification is occurred between the acyl chloride and cholesterol. Similarly, the C=O stretching bands in ester linkages of **M2** are different from those of reactant (3-trifluoromethyl-phenoxy)-acetyl chloride. ^{1}H-NMR and ^{13}C-NMR spectra of **M1** and **M2** were shown in Figure 1, the labeled representing protons and corresponding peak assignments were also illustrated in the figures, which was in good agreement with the prediction.

Polymers **Pa–Pf** were prepared by a one-step hydrosilylation reaction between Si—H groups of PMHS and terminal olefinic group (CH_2=CH—) of **M1** and **M2**. The PMHS was reacted with the olefins (5% in excess versus Si—H groups) in a minimum volume of anhydrous toluene under nitrogen. An excess amount of olefin monomers was usually employed to carry the hydrosilation reaction to completion. The catalyst was employed hexachloroplatinic acid in THF solution, used in high concentration above 65°C, gave good results. The unreacted monomers were removed by several reprecipitations from tetrahydrofuran solution into methanol. Therefore, the polymers were isolated with high purity. In the FTIR spectra, in comparison with the spectra of the reacting material PMHS, the spectra of polymers **Pa–Pf** exhibited the following characteristics: (I) Complete disappearance of Si—H vibration, which was observed near 2160 cm^{-1}; (II) Appearance of C=O bond near 1730 cm^{-1}, benzene ring (—C=C—) near 1600 cm^{-1} and 1500 cm^{-1}, and C—O—C bond near 1170 cm^{-1} due to their stretch vibrations, which are originated from the monomers **M1** and **M2**; (III) Other peaks, i.e. Si—O—Si stretching vibration near 1060 cm^{-1}, Si—CH_3 bending vibration near 840 cm^{-1}, are also observed, which are originated from the reacting material PMHS. All these observations indicate that the Si—H bond disappeared after hydrosilylation; while siloxane group remained, and new chemical groups, such as phenyl, carbonyl, and ether have been formed by hydrosilylation as expected. In the ^{1}H-NMR spectra, signals characteristic of terminal olefinic moiety in the monomers, i.e. δ of CH_2=CH— near 5.44 and 6.05 ppm, were not displayed. On the other hand, the δ of —SiH— on PMHS was shown near 4.68 ppm in the ^{1}H-NMR spectrum, and this peak became weak and disappeared in the process of hydrosilylation action, indicating that all the Si—H in PMHS were substituted. The ^{1}H-NMR spectrum, the labeled protons and corresponding peak assignments of representative polymer **Pc** were displayed in Figure 2. All these results confirms that the monomers were connected to the polysiloxane chains.

For the LC polysiloxanes, it is necessary to know the polymer composition and molecular weights. ^{1}H-NMR studies of the polymers allowed the evaluation of the grafting yield and the purity of the polymers obtained. For PMHS, the substitution degree can be determined by comparison of the integration of the Si-H signals to those of the Si-methyl groups. In order to know the polymer composition, substitution degree of **M1** and **M2** can be determined by comparison of the integration ratio of the —CH_2CH_2O—/Si—CH_3 and —$OOCCH_2O$—/Si—CH_3 signals respectively by ^{1}H-NMR analyses in the polymer systems, because both **M1** and **M2** component showed —CH_2CH_2O— signals, but only **M2** component displayed —$OOCCH_2O$— signals. The δ value of —CH_2CH_2O— and —$OOCCH_2O$— were exhibited near 4.2 and 4.9 ppm, respectively. Therefore, the polymer composition of the polymers and molecular weights could be calculated, which were

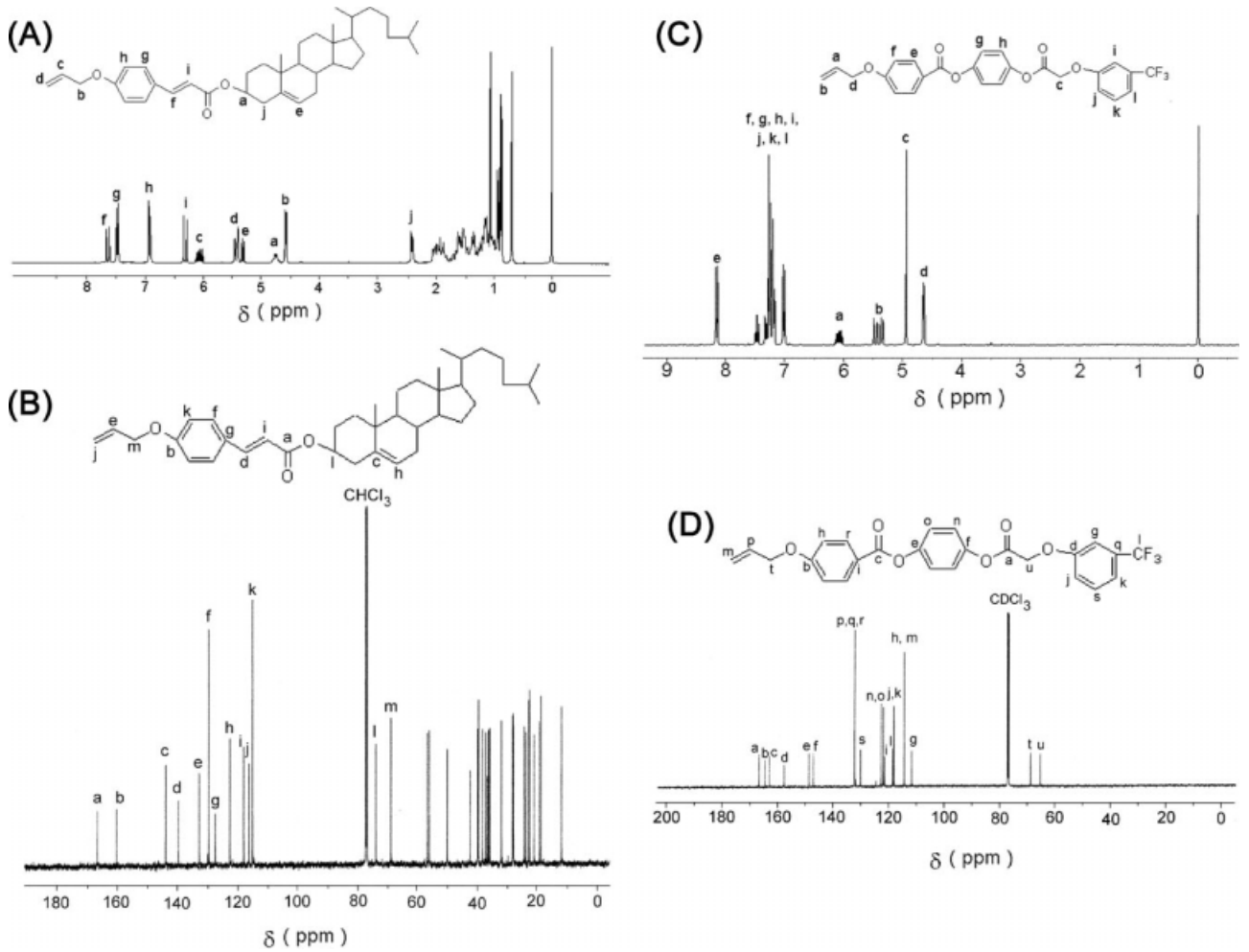

Figure 1 NMR spectra of cholesteryl 3-(4-allyloxy-phenyl)-acryloate (**M1**) and 4-[2-(3-trifluoromethyl-phenoxy)-acetoxy]-phenyl 4-allyloxy-benzoate (**M2**): (A) ^{1}H-NMR spectrum of **M1**; (B) ^{13}C-NMR spectrum of **M1**; (C) ^{1}H-NMR spectrum of **M2**; (D) ^{13}C-NMR spectrum of **M2**.

listed in Table I. Furthermore, both —OOCCH$_2$O— and trifluoromethyl groups are concomitant on the **M2** structure, and the proportion is definite. Therefore, the mass percentage of trifluoromethyl-substituted mesogens in the polymers could be determined according to ^{1}H-NMR spectra analysis, as shown in Table I. It indicated that the M_n of the synthesized polymers decreased slightly with increase of **M2** feed in polymerization.

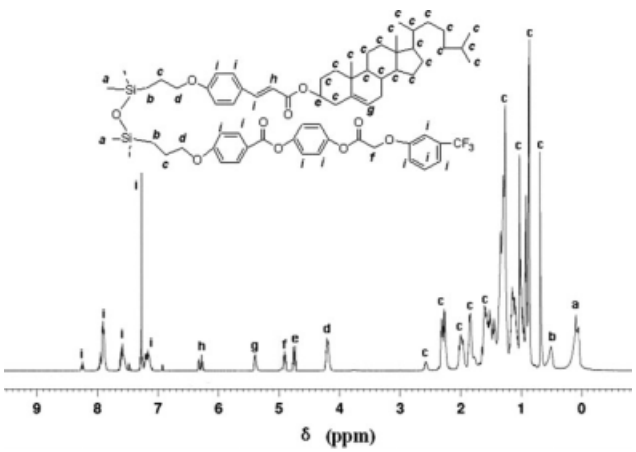

Figure 2 ^{1}H-NMR spectrum of representative polymer **Pc**.

The specific rotations of the liquid crystalline polymers are given in Table I, indicating that the polysiloxanes showed lower specific rotation absolute values in comparison with monomer **M1** ($[\alpha] = -29.5°$). It suggested that cleavage of the terminal olefinic bond and the binding of monomers to the polysiloxane main chains affect the chirality of the polysiloxanes. In addition, the specific rotation of polymers revealed that absolute values decreasing with increase of **M2** component from **Pa** to **Pf**, suggesting the decrease of chiral components.

Liquid crystalline behaviors of monomers

Liquid crystalline behaviors of these olefin monomers were studied using DSC, POM, and XRD, and

TABLE II
Thermogravimetric Analysis, Phase Transitions, and Phase Transition Enthalpies for Monomers and the Series of Polymers

Sample	Thermogravimetric analysis			Phase transitions, °C (corresponding enthalpy changes; J/g)[a]
	T_d[b] (°C)	Inflection[c] (°C)	Residue[d] (%)	Heating / Cooling
M1				C 147.8 (49.22) N^* 251.8 (3.64) I I 222.2 (0.64) N^* 139.2 (31.84) C
M2				C 115.7 (76.15) S_C 172.7 (0.17) I I 171.5 (0.16) S_C 93.5 (49.33) C
Pa	316.1	412.5	5.02	G 6.2 N^* 189.8 (0.45) I I 179.3 (0.16) N^* 15.3 G
Pb	318.7	416.5	5.22	G 11.7 N^* 184.6 (1.22) I I 164.8 (0.29) N^* 15.8 G
Pc	315.2	411.4	5.43	G 12.9 S_A^* 199.1 (0.23) I I 170.9 (0.29) S_A^* 18.9 G
Pd	317.7	407.7	6.28	G 16.8 S_A^* 195.3 (0.25) I I 178.7 (0.17) S_A^* 18.7 G
Pe	313.5	405.8	7.38	G 21.8 S_A^* 202.5 (0.11) I I 178.4 (0.37) S_A^* 19.4 G
Pf	321.9	406.9	8.32	G 29.9 S_A^* 201.6 (0.63) I I 199.8 (0.46) S_A^* 20.8 G

[a] C, crystalline phase; G, glassy; N^*, chiral nematic; S_A^*, smectic A^*; I, isotropic phase.
[b] Temperature of the samples at 5% loss weight.
[c] Inflection temperature of the samples between the two mass changes.
[d] Residue weight of the samples on heating to 600°C.

both **M1** and **M2** exhibited mesomorphic behaviors. The study by DSC enables us to determine the transition temperatures of the monomers. The thermal transition and corresponding enthalpy changes of **M1** and **M2** were summarized in Table II, and the DSC thermograms were displayed in Figure 3. Figure 3(a) presents DSC curves of LC monomer **M1** that contains cholesteryl cinnamate groups. A melting transition at 147.8°C is displayed here, followed by a chiral nematic (N^*) to isotropic phase transition at 251.8°C on the heating cycle. The cooling scan exhibits an isotropic-N^* transition at 222.2°C, and crystallization at 139.2°C. The DSC curves of LC monomer **M2** [Fig. 3(b)] showed a melting transition at 115.7°C, a smectic C (S_C)-isotropic phase transition at 172.7°C on the second heating scan, as well as a isotropic-S_C transition at 171.5°C and crystallization at 93.5°C on the first cooling scan.

Figure 4 presents the typical textures of precursors **M1** and **M2**. The precursor **M1** exhibited enantiotropic chiral nematic (N^*) with oily streak texture and focal conic texture, as shown in Figure 4(a,b). One of the most commonly observed textures of the cholesteric phase prepared between two untreated glass substrates is oily streak texture. The director is basically anchored under planar conditions at the substrates, i.e. with the long molecular axis parallel to the bounding plates, which implies that the cholesteric helix axis is oriented perpendicular to the glass plates.

When **M2** was heated, a mosaic texture appeared firstly [Fig. 4(c)], and domain textures of S_C phase were finally observed between crossed polarizers, as shown in Figure 4(d). The domain texture of S_C phase subjected to planar boundary conditions in a thin sandwich cell. The two types of domains result from the tilt of the director to either side of the smectic layer normal. For S_C phase, the molecules form a lamellar structure, while in an individual smectic layer the centers of mass are isotropically distributed. The director n makes an angle θ that is the so-called 'tilt angle'. Without appropriate boundary conditions the orientation of the director on the tilt cone is arbitrary and not predetermined. Under planar boundary conditions the director n is oriented in the plane of the substrate. The director can no longer take an arbitrary position on the tilt cone θ, but is now confined to the cut between the tilt cone and the substrate plane. This leaves two positions, $+\theta$ and $-\theta$, corresponding to the domain texture.[28] When the isotropic melt was cooled, a texture similar to fan-shaped texture appeared, as shown in Figure 4(e), suggesting the direct isotropic to S_C phase transition.[28] As the sample was cooled continuously, a lined texture was displayed, as shown in Figure 4(f).

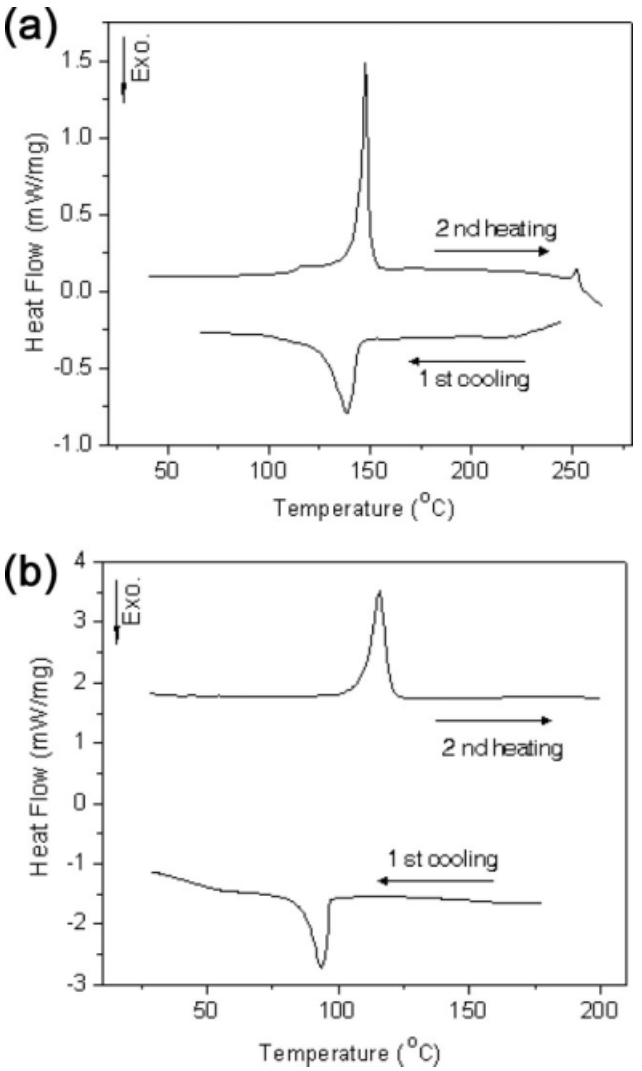

Figure 3 DSC thermograms for (a) cholesteryl 3-(4-allyloxy-phenyl)-acryloate (**M1**); and (b) 4-[2-(3-trifluoromethyl-phenoxy)-acetoxy]-phenyl 4-allyloxy-benzoate (**M2**).

The powder XRD pattern of the high-temperature phases of both **M1** and **M2** showed diffuse peaks in the wide-angle region, but sharp peaks in the small-angle region appeared only for **M2**, suggesting smectic layers of **M2**. All these results indicated that **M1** and **M2** displayed chiral nematic and smectic C mesophase, respectively. For **M2**, the S_C phase with the director being tilted by an angel with respect to the smectic layer should be derived from trifluoromethyl-substituted mesogens in its chemical structure.

Thermal behaviors of polymers

Figure 5 presents TGA thermograms of the polymers, and the TGA data is listed in Table II. It exhibited that the temperatures, at which 5% weight loss occurred (T_d) were greater than 300°C for all the polymers, indicating that they show high thermal stability. All the samples exhibited two mass changes, and the inflection temperature of the samples between the two mass changes decreased slightly with increase of trifluoromethyl-substituted mesogens component in the polymer systems. In addition, the residue weight of the samples on heating near 600°C increased from **Pa** to **Pf**, indicating increased thermal stability with increase of trifluoromethyl-substituted mesogens component in the polymer systems. These TGA results suggested that the trifluoromethyl-substituted mesogens influenced weight loss greatly for these polymers bearing both cholesteryl cinnamate groups and trifluoromethyl-substituted mesogens.

Figure 6 shows DSC thermograms of the polymers on the second heating and the first cooling scan, and the phase transition temperatures and corresponding enthalpy changes of the polymers **Pa–Pf** are summarized in Table II. For all the polymers, when they

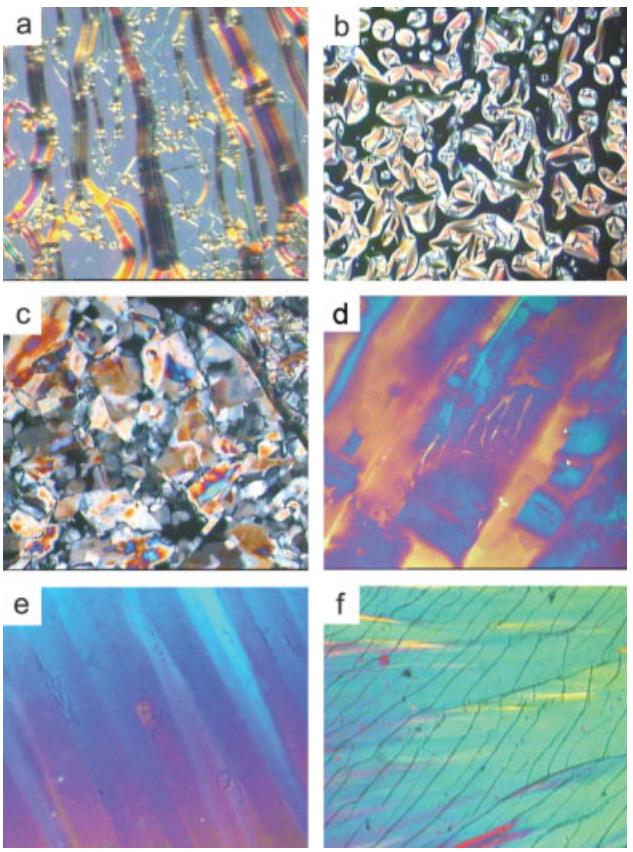

Figure 4 Optical texture of the monomers (200×): (a) oily streak texture of cholesteryl 3-(4-allyloxy-phenyl)-acryloate (**M1**) on heating to 154°C; (b) focal conic texture of **M1** on cooling to 201°C; (c) mosaic texture for 4-[2-(3-trifluoromethyl-phenoxy)-acetoxy]-phenyl 4-allyloxy-benzoate (**M2**) on heating to 117°C; (d) domain texture for **M2** on heating to 151°C; (e) similar to fan-shaped texture of **M2** on cooling to 146°C; (f) lined texture of smectic C for **M2** on cooling to 113°C. [Color figure can be viewed in the online issue, which is available at www.interscience.wiley.com.]

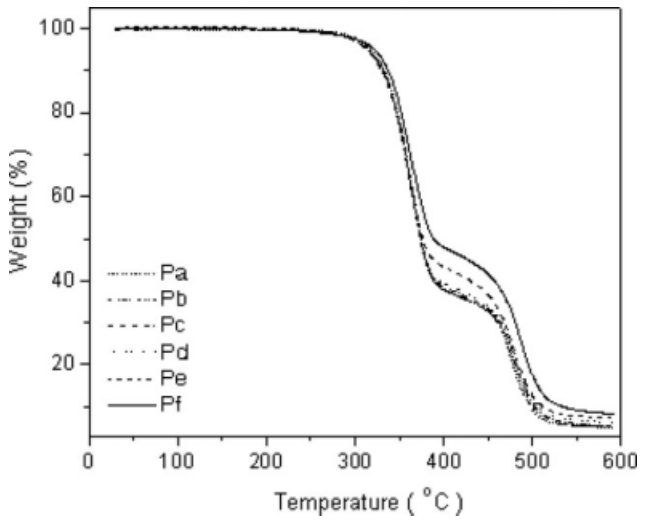

Figure 5 TGA thermograms of the polymers.

were heated, they displayed glass transition and mesophase–isotropic transition; and when they were cooled from melt, they showed isotropic–mesomorphic transitions, and mesomorphic–solid transitions. The temperature of glass transition (T_g) of polymers increased slightly with increase of trifluoromethyl-substituted mesogens in the polymer systems, but isotropic transition temperature (T_i) did not change greatly, showing 170–180°C of mesomorphic temperature range.

These kinds of SCLCPs are composed of flexible moieties (polymer backbone and flexible spacer) and rigid moieties (mesogenic units), thus the polymer backbone, the length of the flexible spacer, the rigidity of mesogenic units, and the interaction generating from trifluoromethyl-substituted mesogens would influence mesophase behaviors of the polymers. The polymer backbones **Pa**–**Pf** are siloxane main chains, thus low temperatures induce vitrification rather than crystallization for these disordered systems of the atactic siloxane polymers. For polymer of this tape, the glass transition may be considered as a measure of the backbone flexibility. In our case, the polysiloxanes were prepared through hydrosilication reaction with poly(methylhydrogeno)siloxane, one monomer (**M1**) containing cholesteryl cinnamate groups, and another monomer (**M2**) containing trifluoromethyl-substituted mesogens. Therefore the backbone flexibility of the polymers is influenced mainly by two factors: the length of the flexible spacer, and the rigid mesogenic units. Although the flexible spacer between polysiloxane main chains and the rigid structures (cholesteryl cinnamate groups and trifluoromethyl-substituted mesogens) are the same, the rigid mesogenic units are different between **M1** and **M2**, resulting in changes of T_g and T_i from **Pa** to **Pf**.

Optical textures and x-ray diffraction analysis of polymers

Figure 7 shows some representative optical textures of the polymers, which were studied by means of POM with hot stage. The polymers **Pa** and **Pb** exhibited N^* textures when they were heated and cooled, but polymers **Pc**, **Pd**, **Pe**, and **Pf** containing more trifluoromethyl-substituted mesogens displayed chiral smectic A (S_A^*) textures. For the sample **Pa**, which contains the most cholesteryl cinnamate groups and no trifluoromethyl-substituted mesogens, when it was heated, eyesight became bright and LC textures appeared, and finally a Grandjean texture was induced under slight shear stress, as shown in Figure 7(a). Under polarizing optical microscopy, the cholesteric mesophase is identifiable with Grandjean textures, depending on the orientation of the axis

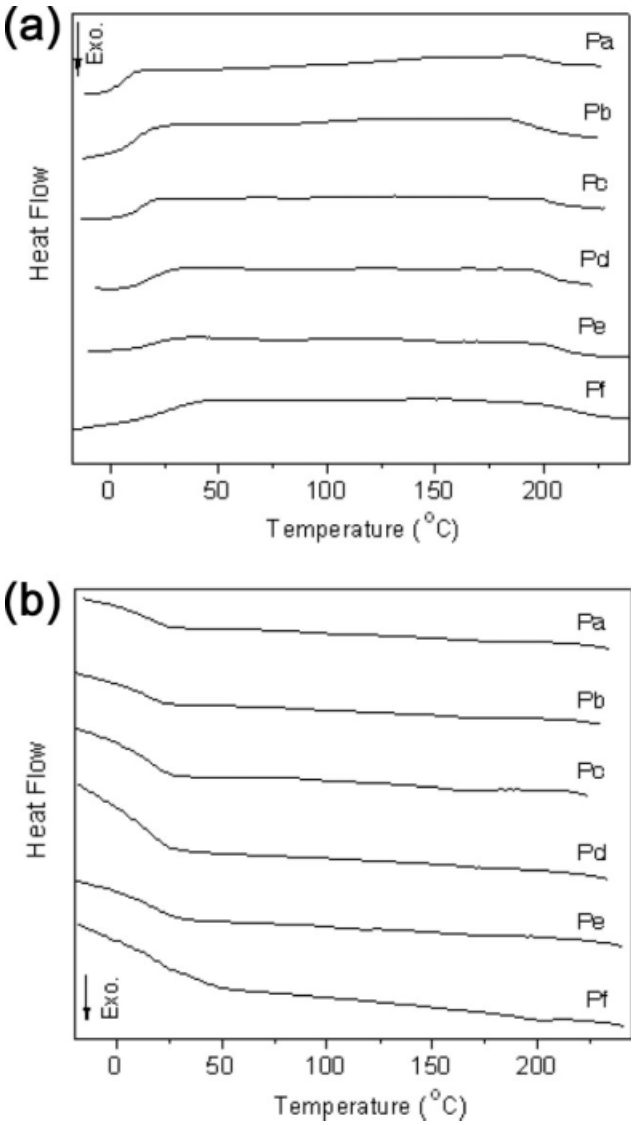

Figure 6 DSC thermograms of polymers: (a) on the second heating cycles; (b) on the first cooling cycles.

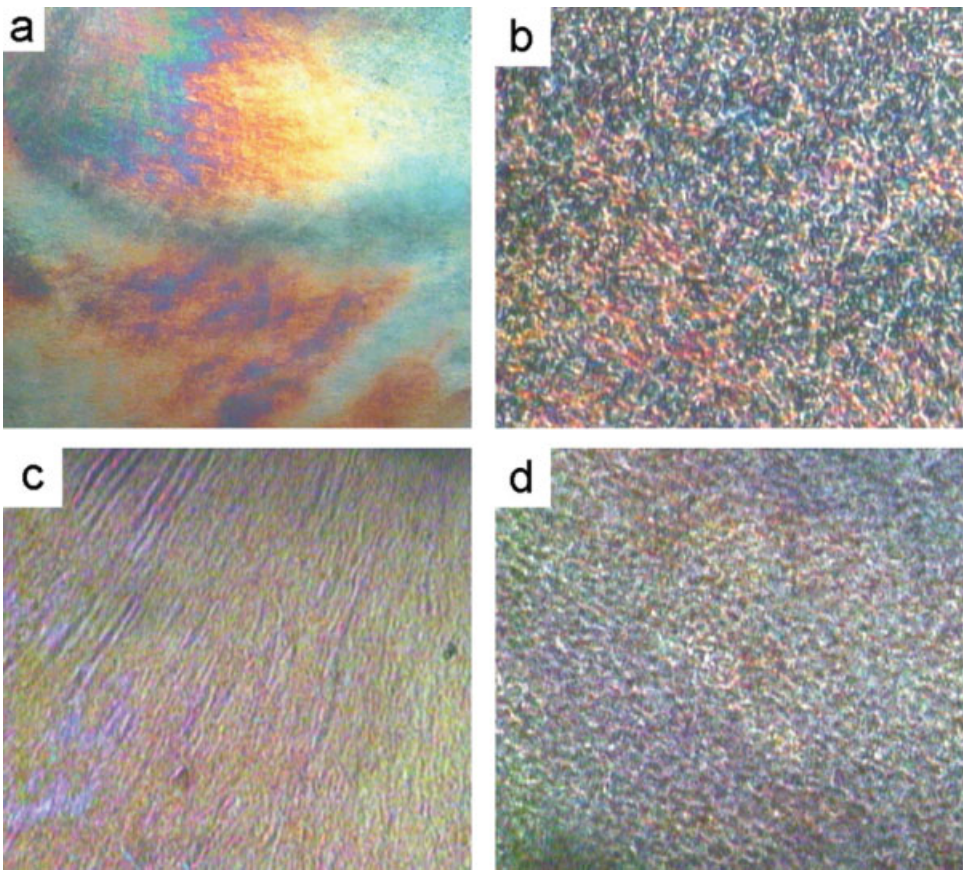

Figure 7 Optical texture of the liquid crystalline polymers (200×): (a) **Pa** on heating to 186°C; (b) **Pa** on cooling to 121°C; (c) **Pf** on heating to 192°C; (d) **Pf** on cooling to 162°C. [Color figure can be viewed in the online issue, which is available at www.interscience.wiley.com.]

with the substrate.[29] In the Grandjean mode, the axis is perpendicular to the substrate with a selective reflection of visible light. When the isotropic melt was cooled, some spherical nuclei were observed to grow from the black background of the isotropic melt, and then focal conic textures appeared gradually, as exhibited in Figure 7(b). The focal conic textures of the polymer were not as distinct as those of small molecule liquid crystals because of high viscosity. For the sample **Pb**, similar textures were exhibited. For the samples **Pc**, **Pd**, **Pe**, and **Pf** that contain a little cholesteryl cinnamate groups and more trifluoromethyl-substituted mesogens, when they were heated and cooled, analogous textures appeared. The sample **Pf** was illustrated as an example. When **Pf** was heated, a striped texture of S_A^* phase emerged instead of Grandjean texture under slight shear stress, as displayed in Figure 7(c). On cooling, some elongated germs appeared firstly in the dark viewing field of the isotropic fluid for **Pf**, and then formed different focal conic textures from **Pa** [Fig. 7(d)], suggesting that isotropic-S_A^* phase transition of **Pf** were easily distinguished from the isotropic-N^* phase transition of **Pa**.

XRD analysis was performed to get more information of the mesophase identification. Table I lists the data from powder XRD studies, which were performed on mechanically oriented samples prepared by shearing at a temperature just below isotropization and suddenly cooling the sample to room temperature. The representative XRD curves of the polymers **Pa**, **Pd,** and **Pf** are shown in Figure 8. XRD curves of samples of **Pa** and **Pb** displayed weak broad reflections in the small-angle region ($2\theta \approx 2.8°$) together with strong diffuse reflection in wide-angle region ($2\theta \approx 16.2°$, d spacing 5.4 Å) that can be ascribed to the distance between the molecules in the LC phase. This is a typical pattern of the N^* phase. But a diffuse reflection at wide angles and a sharp reflection at small angles (associated with the smectic layers) are separately shown by curves of polymers **Pc**, **Pd**, **Pe**, and **Pf**, suggesting S_A^* phase. On the one hand, these diffuse wide-angle reflections became sharp in comparison with **Pa** and **Pb**, indicating the distances between the LC molecules trend to be constant. Besides, the 2θ value of diffuse wide-angle reflection peaks shifted slightly to wide angle, suggesting the lateral spacing of mesogenic

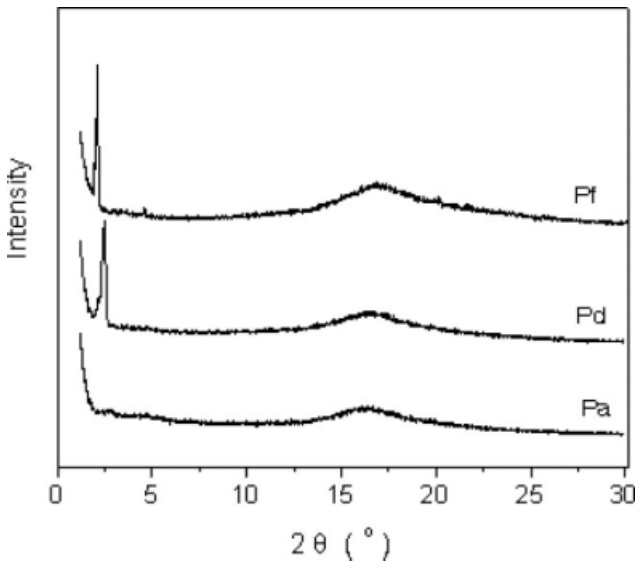

Figure 8 XRD curves of the representative polymers.

side groups became shorter with increase of the trifluoromethyl-substituted mesogens in the polymer systems. On the other hand, the intensity of sharp reflections at low angle increased with increase of trifluoromethyl-substituted mesogens in the polymers systems, indicating strengthening smectic layer structures.

The SCLCPs are composed of flexible and rigid moieties, self-assembly and nanophase separation into specific micro-structures frequently occur due to geometric and chemical dissimilarity of the two moieties. For all the polymers, the flexible moieties include the siloxane main chains and the flexible alkyl spacer groups, and the rigid moieties are constituted from the cholesteryl cinnamate mesogens and the trifluoromethyl-substituted mesogens. Because both **M1** and **M2** comprise terminal allyloxy groups that were combined to polysiloxane main chains via hydrosilylation, the flexible moieties are the same for all the polymers. Thus the differences of structures and properties of the SCLCPs are derived from the rigid moieties, i.e. the cholesteryl cinnamate mesogens and the trifluoromethyl-substituted mesogens in the polymer systems.

Fluorine's small size, large electronegativity, low polarizability, and large fluorine–fluorine repulsion lead to many interesting properties of fluoropolymers. For the sample **Pa**, which contains no fluorinated units, the cholesteric mesophase should be induced due to chiral building block of the cholesteryl cinnamate mesogens. These chiral mesogens would be embedded in flexible moieties of the polymer matrix, thus the helix structure should be formed. This is confirmed by the XRD analysis, i.e. the sample **Pa** displayed weak broad reflections in the small-angle region. No strong peaks appeared at the small angles suggesting no layer package in this case. With increase of trifluoromethyl-substituted mesogens in the polymer systems, the structures and properties of the polymers would be varied due to the introduction of fluorine-containing units. There would exist some repulsion between fluorinated tails and the polymer matrix (constituted by polysiloxane main chains and the hydrocarbons) because of the fluorophobic effect, leading to rearrangement fo mesogens order within the polymer matrix. On the other hand, the trifluoromethyl-substituted mesogens would aggregate themselves as a result of fluorophilic effect. Thus the lamellar structure could be formed to exhibit S_A^* mesophase, and the N^* mesophase could be restrained. Schematic arrangements of the cholesteryl cinnamate mesogens and trifluoromethyl-substituted mesogens in the series of polymers are displayed in Figure 9. Furthermore, with increase of trifluoromethyl-substituted mesogens from **Pc** to **Pf**, thickness and intension of the smectic layers became would be enlarged, which was in agreement with the XRD analysis.

CONCLUSIONS

We synthesized a cholesteric LC monomer cholesteryl 3-(4-allyloxy-phenyl)-acryloate and a fluoro-

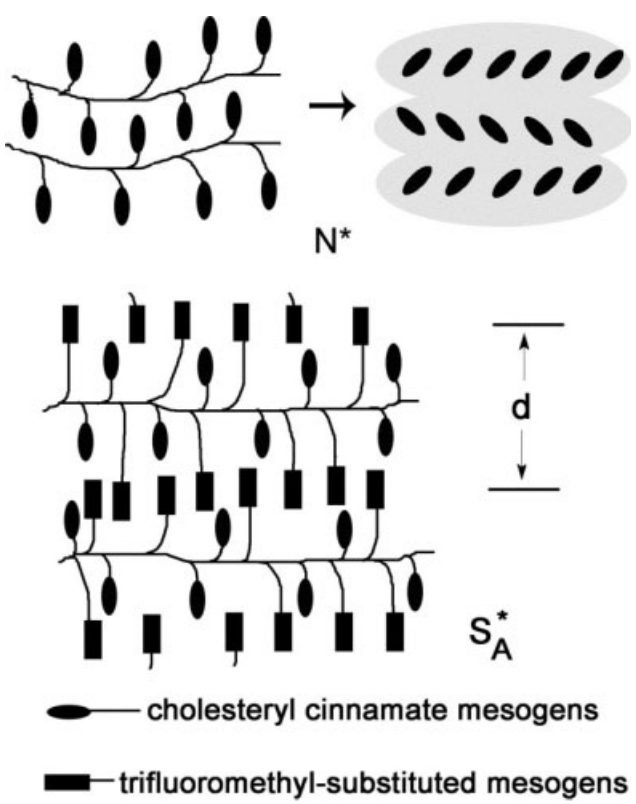

Figure 9 Schematic arrangements of the cholesteryl cinnamate mesogens and trifluoromethyl-substituted mesogens in the series of polymers.

containing LC monomer 4-[2-(3-trifluoromethyl-phenoxy)-acetoxy]-phenyl 4-allyloxy-benzoate. By use of these two monomers and poly(methylhydrogeno) siloxane, we prepared a series of side-chain LC polysiloxanes (**Pa**–**Pf**) bearing cholesteryl cinnamate mesogens and trifluoromethyl-substituted mesogens. The chemical structures, composition, and molecular weights were characterized with FTIR, ^{1}H-NMR, ^{13}C-NMR, and XRD. Thermal behaviors of the fluorinated LC polysiloxanes were characterized by use of TGA and DSC. It exhibited that the temperatures at which 5% weight loss occurred were greater than 300°C for all the polymers, and the residue weight of the samples near 600°C increased slightly with increase of trifluoromethyl-substituted mesogens component in the polymer systems, indicating that they show high thermal stability. The T_g of polymers increased slightly with increase of trifluoromethyl-substituted mesogens from **Pa** to **Pf**, but the T_i did not change greatly. The samples **Pa** and **Pb** showed chiral nematic phase, but the samples **Pc**, **Pd**, **Pe,** and **Pf** containing more trifluoromethyl-substituted mesogens exhibited smectic A* phase. The smectic mesophase of the polymers was also characterized by XRD analysis. XRD curves of samples of **Pc**, **Pd**, **Pe,** and **Pf** displayed sharp and strong peaks at low angle together with a strong broad peak in wide angle. Curves of **Pa** and **Pb** exhibited a diffuse reflection in wide angle corresponding to the lateral spacing of two mesogenic side groups, but no sharp reflection at low angle, suggesting no smectic layer structure. Furthermore, the intensity of sharp reflections at low angle increased with increase of trifluoromethyl-substituted mesogens in the polymers systems for **Pc**, **Pd**, **Pe,** and **Pf**, indicating strengthening smectic layer structure. These results should be due to the fluorophobic effect between trifluoromethyl-substituted mesogens and the polymer matrix.

References

1. Cojocariu, C.; Rochon, P. Macromolecules 2005, 38, 9526.
2. Medvedev, A. V.; Barmatov, E. B.; Medvedev, A. S.; Shibaev, V. P. Macromolecules 2005, 38, 2223.
3. Okano, K.; Shishido, A.; Ikeda, T. Adv Mater 2006, 18, 523.
4. Beyer, P.; Krueger, M.; Giesselmann, F.; Zentel, R. Adv Funct Mater 2007, 17, 109.
5. Hsiue, G. H.; Lee, R. H.; Jeng, R. J. Polymer 1997, 38, 887.
6. Hattori, H.; Uryu, T. J Polym Sci Part A: Polym Chem 2000, 38, 887.
7. Chai, C. P.; Zhu, X. Q.; Wang, P.; Ren, M. Q.; Chen, X. F.; Xu, Y. D.; Fan, X. H.; Ye, C.; Chen, E. Q.; Zhou, Q. F. Macromolecules 2007, 40, 9361.
8. Sato, M.; Nakashima, S.; Uemoto, Y. J Polym Sci Part A: Polym Chem 2003, 41, 2676.
9. Sun, S. J.; Schwarz, G.; Kricheldorf, H. R.; Chang, T. C. J Polym Sci Part A: Polym Chem 1999, 37, 1125.
10. Kricheldorf, H. R.; Krawinkel, T. Macromol Chem Phys 1998, 199, 783.
11. Kricheldorf, H. R.; Sun, S. J.; Chen, C. P.; Chang, T. C. J Polym Sci Part A: Polym Chem 1997, 35, 1611.
12. Hsu, L. L.; Chang, T. C.; Tsai, W. L.; Lee, C. J Polym Sci Part A: Polym Chem 1997, 35, 2843.
13. Hsiue, G. H.; Lee, R. H.; Jeng, R. J.; Chang, C. S. J Polym Sci Part B: Polym Phys 1996, 34, 555.
14. Hiraoka, K.; Stein, P.; Finkelmann, H. Macromol Chem Phys 2004, 205, 48.
15. Crevoisier, G. D.; Fabre, P.; Leibler, L.; Tence-Girault, S.; Corpart, J. M. Macromolecules 2002, 35, 3880.
16. Gopalan, P.; Andruzzi, L.; Li, X.; Ober, C. K. Macromol Chem Phys 2002, 203, 1573.
17. Galli, G.; Gasperetti, S.; Bertolucci, M.; Gallot, B.; Chiellini, F. Macromol Rapid Commun 2002, 23, 814.
18. You, F.; Paik, M. Y.; Hackel, M.; Kador, L.; Kropp, D.; Schmidt, H. W.; Ober, C. K. Adv Funct Mater 2006, 16, 1577.
19. Chung, T. S.; Ma, K. X.; Cheng, S. X. Macromol Rapid Commun 2001, 22, 835.
20. Bracon, F.; Guittard, F.; Givenchy, E. T.; Cambon, A. J Polym Sci Part A: Polym Chem 1999, 37, 4487.
21. Goto, H.; Dai, X.; Narihiro, H.; Akagi, K. Macromolecules 2004, 37, 2353.
22. Al-Hussein, M.; Serero, Y.; Konovalov, O.; Mourran, A.; Moller, M.; De Jeu, W. H. Macromolecules 2005, 38, 9610.
23. Goto, H.; Dai, X.; Ueoka, T.; Akagi, K. Macromolecules 2004, 37, 4783.
24. Keith, C.; Dantlgraber, G.; Reddy, R. A.; Baumeister, U.; Tschierske, C. Chem Mater 2007, 19, 694.
25. Dai, X. M.; Goto, H.; Akagi, K.; Shirakawa, H. Synth Met 1999, 102, 1289.
26. Meng, F. B.; Sun, Y. H.; Gao, Y. M.; Song, X. G.; Zhang, B. Y. Polym Adv Technol 2008, 19, 1242.
27. Meng, F. B.; Zhang, B. Y.; Zhou, A. J.; Li, X. Z. J Appl Polym Sci 2007, 104, 1161.
28. Dierking, I. Textures of Liquid Crystals; WILEY-VCH GmbH & Co. KgaA: Weinheim, 2003; pp 91–96.
29. Katsis, D.; Chen, P. H. M.; Mastrangelo, J. C.; Chen, S. H. Chem Mater 1999, 11, 1590.